Int. J. Electrochem. Sci., 17 **(2022)** Article Number: 22066, doi: 10.20964/2022.05.32

International Journal of
ELECTROCHEMICAL
SCIENCE
www.electrochemsci.org

Zn/N co-doped TiO_2 Nanotubes for Enhancement of Photocatalytic Degradation of Pentachlorophenol

Hong Xing[*], *Lihong Wu, Xiaohui Li*

Department of Biomedical and Chemical Engineering, Liaoning Institute of Science and Technology, Benxi 117004
[*]E-mail: xxinggg68@sina.com

Received: 10 January 2021 / *Accepted:* 10 March 2022 / *Published:* 7 May 2022

The purpose of this research was to synthesize mono-doped (Zn/TiO_2, N/TiO_2) and co-doped TiO_2 (Zn/N co-doped TiO_2) nanotubes by the sol-gel method and use them as photocatalysts for the photocatalytic degradation of pentachlorophenol (PCP). Structural analyses by SEM and XRD indicated successful mono-doping and co-doping of TiO_2 nanotubes, and optical studies by UV–vis absorption spectra revealed that the optical band gap values of TiO_2, Zn/TiO_2, N/TiO_2 and Zn/N co-doped TiO_2 nanotubes were estimated at 3.29, 3.25, 3.21 and 3.16 eV, respectively, indicating the band gap of TiO_2 decreased after mono-doping and co-doping with N and Zn. The results of the EIS analyses showed that Zn/N co-doped TiO_2 nanotubes with the lowest charge transfer resistance towards pure and mono-doped TiO_2 can accelerate the interfacial photo-excited charge carrier transfer rate. Studying the photocatalytic activity of the prepared photocatalyst for degradation of 50 ml of 40 mg/l PCP solution upon simulated solar light irradiation showed that the time required of TiO_2, N/TiO_2, Zn/TiO_2 and Zn/N co-doped TiO_2 nanotubes for complete degradation of PCP molecules were 250, 200, 185 and 155 minutes, respectively. The highest rate of photodegradation of PCP solution was observed for the co-doped TiO_2 nanotubes due to the formation of an intermediate band in the energy band-gap of co-doped TiO_2, which has a beneficial synergistic effect by lowering the recombination of photo-excited carriers and increasing visible light absorption.

Keywords: mono-doping; co-doping; Zn, N co-doped TiO_2, nanotubes; sol-gel, Photodegradation; Pentachlorophenol

1. INTRODUCTION

Pentachlorophenol *(*PCP, C_6HCl_5O*)* or Pentachlorol, also known as Santophen, is a synthetic polychlorinated compound with a sharp chemical odor [1, 2]. PCP is used as a pesticide and a disinfectant in wood industrials and the synthesis of herbicides, insecticides, fungicides, algaecides, and disinfectants [3, 4]. It has also been used to protect against mould, fungus, and bacteria in the

leather and textile industries [5-7]. Most industries use this cause to introduce PCP into the environment by wastewaters. The presence of PCP causes water quality problems in effluents and is a major concern due to its toxic effects [8-10].

PCP is toxic to mammals, humans and the environment, in particular to aquatic organisms. Short-term exposure to PCP reveals its toxic effect on the liver, kidneys, and central nervous system [11-13]. Long-term exposure can cause carcinogenic, renal, and neurological effects. Accordingly, it is now a restricted use pesticide and is no longer available to the general public, and it is banned under the United Nation's Stockholm Convention on Persistent Organic Pollutants [14-16].

Thus, there is a great need to verify surface water quality, especially when even just 1.0 mg/l of PCP concentration in drinking water can be quickly absorbed through the gastrointestinal tract following ingestion [17-19]. As a result, determining and degrading PCP in drinking water and wastewater is critical. Electro-Fenton process [20], bioadsorption and biological treatment [21], enzymatic oxidation [22], and photoelectrocatalytic degradation [23-26] are the most used methods for treatment of PCP in water. Among them, photoelectrocatalytic degradation is low-cost, non-toxicity, strong oxidizing power and great chemical stability, and can be applied for the degradation of a wide range of organic and inorganic pollutants [27]. Furthermore, the use of a suitable semiconductor, the synthesis of nanostructured photocatalysts, and doping all increase the rate of degradation. Therefore, this study was focused on the synthesis of Zn/N co-doped TiO_2 nanotubes and their application for photocatalytic degradation of PCP. To the best of our knowledge, there are no previous reports on the Zn/N co-doped TiO_2 nanotubes and their application to the photocatalytic degradation of PCP.

2. EXPERIMENTAL

2.1. Preparation of Zn/N co-doped TiO_2 nanotubes

The nanotubes of TiO_2, Zn/TiO_2, N/TiO_2 and Zn/N co-doped TiO_2 were synthesized by the sol-gel method [28, 29]. The tetrabutyl titanate (97%, Shandong Pulisi Chemical Co., Ltd., China), ammonium chloride (99.5%, Shandong Pulisi Chemical Co., Ltd., China) and $Zn(NO_3)_2{\cdot}6H_2O$ (99%, Shandong Pulisi Chemical Co., Ltd., China) were used as precursors. For preparation of TiO_2 nanotubes, 4.0 mL of tetrabutyl titanate was added to 20 mL of anhydrous ethanol, and the mixture was carefully stirred for 20 minutes to obtain a homogeneous gel. Next, 10 mL of deionized water was gradually added to the sol. Subsequently, the pH of the mixture was adjusted to pH 3 with the addition of acetic acid (99.8%, Shandong Dexiang International Trade Co., Ltd., China) under magnetic stirring for 2 hours until the transparent solution was achieved, which was left at room temperature for 24 hours to obtain a stable suspension of TiO_2 nanotubes. The products were washed with deionized water, filtered and dried in an oven at 65 °C for 3 hours. Afterwards, the TiO_2 nanotubes were calcined in an oven at 400°C for 3 3 hours. For preparation of mono-doped TiO_2 (Zn/TiO_2, N/TiO_2) and co-doped TiO_2 (Zn/N co-doped TiO_2) photocatalysts, the required amounts of ammonium chloride as N source and $Zn(NO_3)_2{\cdot}6H_2O$ as Zn source were added to titanium solution in 5 and 10 %wt, respectively.

2.2. Characterizations

The surface morphology and structural characterizations of synthesized pure and doped TiO_2 nanotubes were investigated using a scanning electron microscope (SEM) and an X-ray diffractometer (XRD, DX-2500, CuKα radiation (λ=1.5414Å), respectively. UV–vis spectrophotometer was used for measuring the UV–vis absorption spectra of samples.

The electrochemical impedance spectroscopy (EIS) measurements was carried out on an electrochemical workstation (CHI660E, Chenhua Technology Co., Ltd., Shanghai, China) with electrochemical cell which consisting modified TiO_2, Zn/TiO_2, N/TiO_2 or Zn/N co-doped TiO_2 electrode as working electrode, a saturated Ag/AgCl electrode as a reference and a platinum as counter electrode. The EIS data was obtained in a frequency range from 10^{-1}-10^5 Hz in a 0.2M Na_2SO_4 (Hubei Aging Chemical Co., Ltd., China) solution with AC amplitude of 5 mV, and ZsimpWin software was used to fit the EIS data. For preparation of TiO_2, Zn/TiO_2, N/TiO_2 or Zn/N co-doped TiO_2 modified GCE, 0.5 mL of dimethylformamide is ultrasonically added to 20 mg/ml of prepared pure, doped and co-doped TiO_2 suspension. Then 5 μL of the products were dropped onto a clean GCE surface, and the modified electrodes were allowed to dry at room temperature.

The photocatalytic performance of all the pure and doped TiO_2 nanotubes was investigated by the photodegradation of 50 ml of PCP solution under light irradiation at room temperature. The photocatalyst amount in the PCP solution was 20 mg. A Xenon lamp (150 W) located at the top of the device was used as source of solar light. Before irradiation light, the mixture of PCP solution and photocatalysts was stirred for 60 minutes in the dark to reach an adsorption-desorption equilibrium between the photocatalyst and PCP molecules. The distance between the light source and surface of solution was kept constant at 5cm. After irradiation light at regular time intervals, PCP solutions were taken. The concentration of the irradiated PCP solutions was determined using UV–vis adsorption spectra which normalized the absorption band intensity of PCP at 220 nm [30, 31]. The photocatalytic degradation efficiency was calculated as the equation (1) [32, 33]:

$$\text{Degradation efficiency (\%)} = \frac{C_0 - C_t}{C_0} \times 100 = \frac{I_0 - I_t}{I_0} \times 100 \qquad (1)$$

Where C_o and C_t are the initial concentration and concentration of degraded PCP solution at time t, respectively, and I_o and I_t are the corresponding absorbance intensities of PCP solutions.

3. RESULTS AND DISCUSSION

3.1. SEM and XRD studies

SEM images of TiO_2 and Zn/N co-doped TiO_2 nanotubes are given in Figure 1. As observed from Figure 1, pure and doped TiO_2 nanotubes randomly form highly porous fibrous networks, which are straight, smooth, and uniform long tubes, and their diameters are 190nm and 240nm for TiO_2 and Zn/N co-doped TiO_2 nanotubes, respectively. Similar diameters increased with the addition of dopant in the TiO_2 nanostructure. Similar observations have been reported in previous studies of doped TiO_2 nanotubes [34-37].

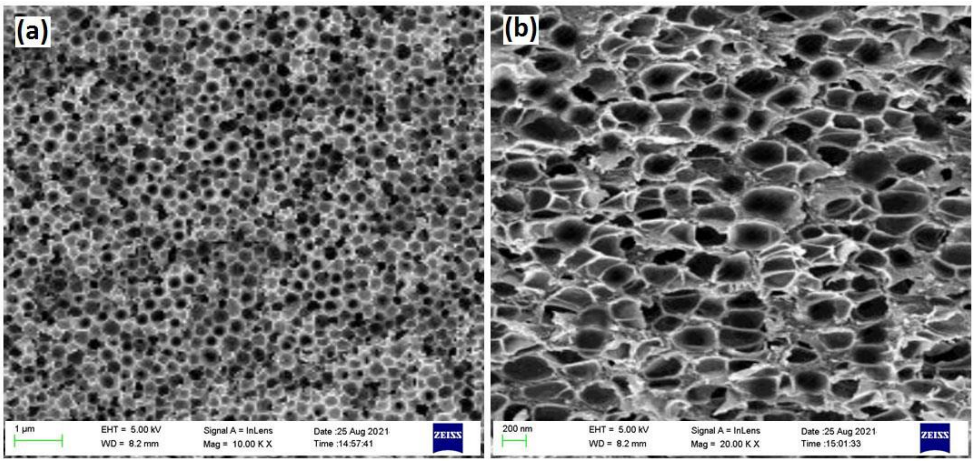

Figure 1. SEM images of (a) TiO_2, (b) Zn/N co-doped TiO_2 nanotubes.

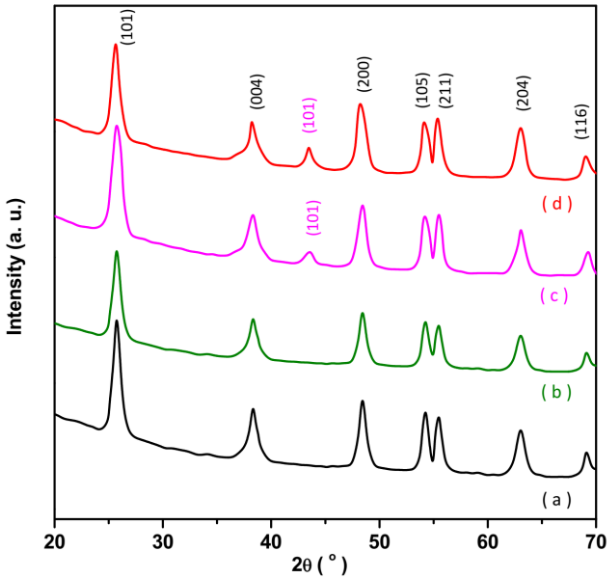

Figure 2. XRD spectra of (a) TiO_2, (b) N/TiO_2, (c) Zn/TiO_2 and (d) Zn/N co-doped TiO_2 nanotubes.

The XRD spectra of TiO_2, N/TiO_2, Zn/TiO_2, and Zn/N co-doped TiO_2 nanotubes are given in Figure 2. As observed from Figure 2a, there are the sharp diffraction peaks at 25.66°, 38.29°, 48.49°, 54.28°, 55.43°, 62.98° and 698.99° signed to the anatase phase of TiO_2, corresponding to (101), (004), (200), (105), (211), (204) and (116) planes, respectively (JCPDS card files, no. 21–1272). Any peaks related to N dopant are not observed in the XRD spectra of N/TiO_2. XRD spectra of Zn/TiO_2 and Zn/N co-doped TiO_2 show one additional weak peak at 43.48° which is related to the (101) plane of metallic Zn with crystallographic phase of face centered cubic (fcc) (JCPDS card files, no. 00-004-0831). However, the (101) peak of Moreover, (101) anatase TiO_2 showed a slight peak shifting towards

lower diffraction angle because of incorporation Zn ions in TiO_2 lattice, inducing substitution of Zn ions with smaller ionic radius (0.60 Å) into Ti^{4+} ions (0.68 Å) in anatase TiO_2 [38-40].

3.2. Optical study

UV–vis spectra and Tauc plot of $(\alpha h\upsilon)^2$ vs $(h\upsilon)$ of TiO_2, N/TiO_2, Zn/TiO_2 and Zn/N co-doped TiO_2 nanotubes are shown in Figure 3. In Figure 3a, the red shift of the light absorption edge of doped TiO2 nanotubes is observed as compared to the undoped sample in absorption spectra. The degree of red shift increases for co-doped TiO_2 nanotubes. The red shift of the edge of absorption spectra is associated with the narrower band gap energy. In Figure 3b, the x-axis intersection point of the linear fit of the Tauc plot gives an estimate of the optical band gap energy [38, 41]. The obtained optical band gap values of TiO_2, Zn/TiO_2, N/TiO_2 and Zn/N co-doped TiO_2 nanotubes are 3.29, 3.25, 3.21 and 3.16 eV, respectively. The optical band gap value of the undoped sample is near to the anatase phase's predicted value (3.2 eV) [42]. The band-gap of TiO_2 reduces after Zn doping, which is consistent with prior studies of Zn doped TiO_2 [43, 44]. This reduction in band gap is due to the formation of Ti-O-Zn bonds and a lower Fermi level of Zn than that of TiO_2 [43, 45]. In order to adjust the Fermi energy levels, electrons have a tendency to flow from higher to lower Fermi levels. Thus, Zn can accept the photo-excited electrons from TiO_2.

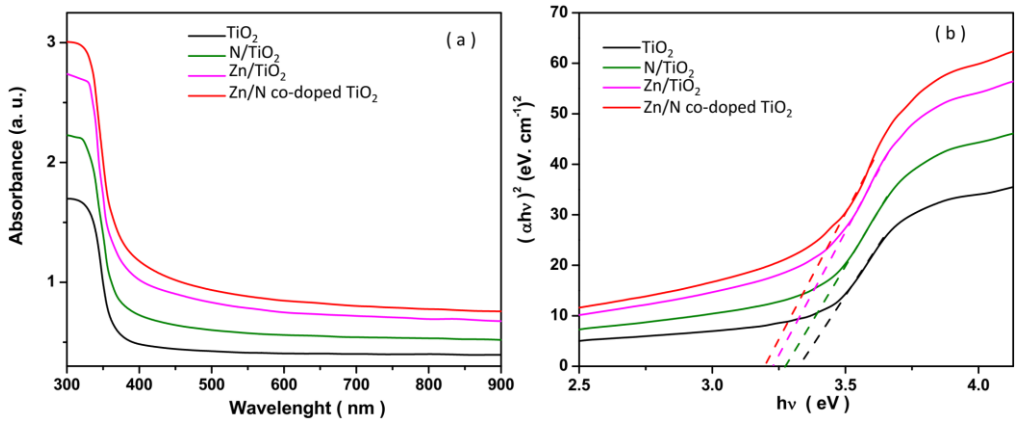

Figure 3. (a) UV–vis spectra and (b) Tauc plot of $(\alpha h\upsilon)^{1/2}$ vs $(h\upsilon)$ of TiO_2, N/TiO_2 Zn/TiO_2, and Zn/N co-doped TiO_2 nanotubes.

Thus, the photo-excited electron-hole pairs get effectively separated, and as a consequence, electron-hole recombination can be decreased [43]. Because of the creation of distinct levels above the valance band edge after N doping, the band-gap of TiO_2 drops to 3.25 eV, which is connected to substitutional nitrogen influence in the band structure by mixing N-2p and O-2p states [46]. The Zn/N co-doped TiO_2 nanotubes show the minimum ban gap which indicates beneficial use of solar spectra. It evidences the easier generation of electronic transitions under the excitation of light [29], and is attributed to sub-band transitions closely related to the surface oxygen vacancies [44, 47]. It is implied

that co-doping of the N and Zn elements could have a synergistic effect and enhance the photocatalytic activity of Zn/N co-doped TiO_2 nanotubes.

3.3. EIS analysis

In order to study the charge transfer rate at the photocatalyst/electrolyte interface among the TiO_2, N/TiO_2, Zn/TiO_2 and Zn/N co-doped TiO_2 nanotubes, the results of EIS and bode plots, and the used equivalent circuit are displayed in Figure 4. The equivalent circuit consists of Rs and R1 as solution resistance and electrolytic resistance, respectively, Rct also corresponds to charge transfer resistance, and Q demonstrates the electrochemical double-layer capacitance [48, 49]. The radius of the incomplete semicircle on the Nyquist plot indicates the value of charge transfer resistance and the charge separation ability [50, 51]. Table 1 summarizes the results obtained for fitting data of circuit elements. As observed, the value of Rct shows an obvious decrease with the mono-doping and co-doping of N and Zn, and the Zn/N co-doped TiO_2 nanotubes has the lowest charge transfer resistance, which indicates the higher charge transfer resistance and the charge separation ability of Zn/N co-doped TiO_2 nanotube toward the TiO_2, N/TiO_2, Zn/TiO_2 samples, and as consequence, highly efficient photocatalyst performance of Zn/N co-doped TiO_2 nanotube.

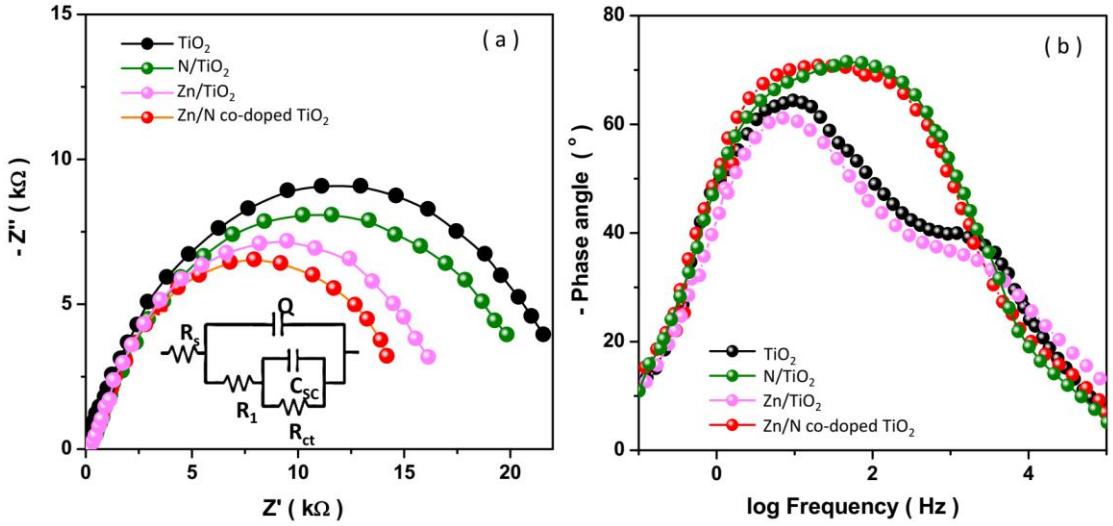

Figure 4. Results of (a) EIS analyses and used equivalent circuit, and (b) Bode plots.

Table 1. The resulted values for fitting data of the circuit elements.

Sample	Rs(Ω)	R_1(Ω)	C_{cs} (μF)	R_{ct} (kΩ)
TiO_2	42.31	48.31	9.721	22.50
N/TiO_2	49.77	48.40	10.821	21.33
Zn/TiO_2	16.29	17.41	16.240	17.55
Zn/N co-doped TiO_2	13.95	15.72	20.353	15.014

3.4. Study the photocatalytic activity

The photocatalytic activity of TiO_2, N/TiO_2, Zn/TiO_2 and Zn/N co-doped TiO_2 nanotubes was compared for the photodegradation of 50 ml of 40 mg/l PCP solution upon simulated solar light irradiation (Figure 5). The sample without a photocatalyst (blank) shows the photodegradation less than 3% after 250 minutes of light irradiation. As seen, the time required for TiO_2, N/TiO_2, Zn/TiO_2 and Zn/N co-doped TiO_2 nanotubes for complete degradation of PCP molecules are 250, 200, 185 and 155 minutes, respectively. The highest rate for photodegradation of PCP solution is observed for the co-doped TiO_2 nanotubes, indicating higher absorption ability and the necessary to finish the reaction with a minimum time compared with the other samples. Generally, the photocatalytic process mainly involves the steps of electron-hole pairs upon light irradiation, separation, recombination, and surface capture of photo-excited electrons and hole pairs [52]. The photo-excited electrons can be excited from the valence band to the conduction band, leaving behind a positive vacancy hole (h^+) which participates in redox reactions with adsorbed species and strongly oxidize molecules of pollutants [53]. The co-doping of N and Zn atoms can improve the photodegradatin rate of TiO_2 under visible light because the metal dopant creates more electron trap centers [54-56], and oxygen vacancies act as catalytic centers that facilitate the charge carriers transport to the surface reactive sites and improve absorption of visible light by virtue of their reduced optical band gaps [57, 58]. Moreover, the porous structures of nanotubes provide large surface area and promote adsorptive and reactive sites and catalyze the photocatalytic performance in the visible light region, enhancing a photodegradation efficiency [57, 59, 60]. These results are in agreement with the results of optical and EIS analyses.

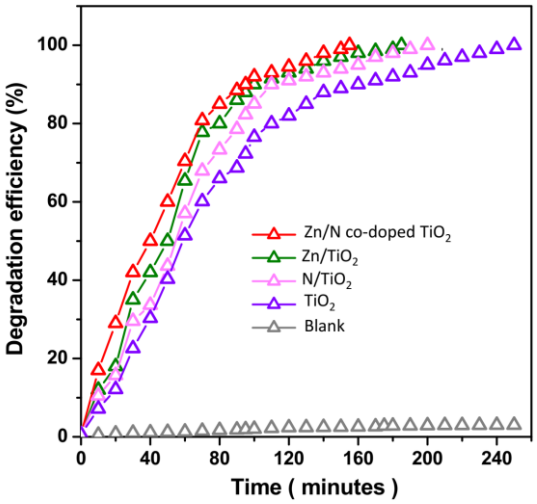

Figure 5. The photocatalytic activity of TiO_2, N/TiO_2, Zn/TiO_2 and Zn/N co-doped TiO_2 nanotubes for photodegradation of 50 ml of 40 mg/l PCP solution upon simulated solar light irradiation.

Figure 6 depicts the photocatalytic degradation activity of Zn/N co-doped TiO_2 nanotubes for the treatment of 50 ml of 2, 10, 20, 40 and 100 mg/l PCP solution upon simulated solar light irradiation. It is observed that complete photodegradation of 2, 10, 20, 40 and 100 mg/l PCP solution is

achieved after 90, 100, 125, 155 and 220 minutes of light irradiation, respectively. With the increase in the initial PCP concentration, catalyst surfaces get covered/saturated for a fixed amount of photocatalyst. Therefore, at higher PCP concentrations, the photodegradation rate decreases.

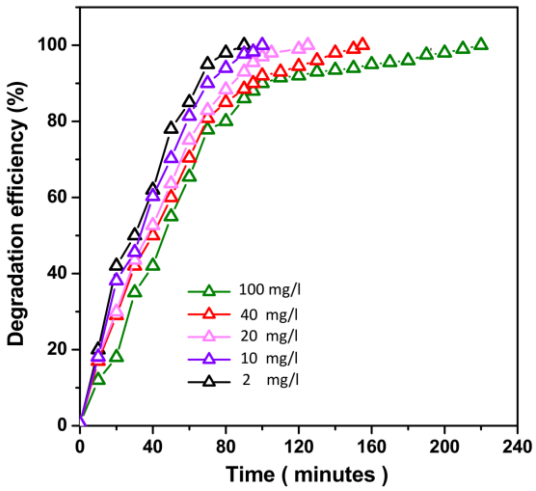

Figure 6. The photocatalytic degradation activity of Zn/N co-doped TiO_2 nanotubes for treatment of 50 ml of 2, 10, 20, 40 and 100 mg/l PCP solution upon simulated solar light irradiation.

Table 2. The comparison between photocatalytic activities of Zn/N co-doped TiO_2 nanotubes with other reported photocatalysts for degradation of PCP.

Photocatalyst	PCP **content (mg/l)**	**Light source**	**Degradation time (minute)**	**Degradation efficiency (%)**	**Ref.**
Zn/N co-doped TiO_2 nanotubes	2	Simulated solar light	90	100	This work
	10		100		
	20		125		
	40		155		
	100		220		
Bii_2SiO_{20}	2	Simulated sunlight	120	99.1	[23]
Cu/ZnS	8	Simulated sunlight	120	68.4	[23]
$ZnSe/TiO_2$	10	Solar light	120	86.2	[25]
Zn-doped TiO_2 nanotubes	10	Solar & visible light	300	88	[24]
TiO_2	10	UV	960	100	[61]
TiO_2 nanotubes	20	UV	120	62	[62]
TiO_2/SiO_2	40	UV–vis	20	93.5	[63]

The comparison between the photocatalytic activities of Zn/N co-doped TiO_2 nanotubes with other reported photocatalysts for degradation of PCP is presented in Table 2. It can be found that Zn/N

co-doped TiO_2 nanotubes show effective performance for photodegradation of PCP upon simulated solar light due to the formation of an intermediate band in the energy band-gap of co-doped TiO_2, which creates a beneficial synergistic effect by lowering recombination of photo-excited carriers and higher visible light absorption.

The applicability of Zn/N co-doped TiO_2 nanotube for photodegradation of PCP in a prepared real sample of agricultural wastewater was studied. As observed from Figure 7, the comparison between UV–Vis spectra for degradation of 50 ml of 10 mg/l PCP solution prepared in a real sample of agricultural wastewater and prepared in deionized water using Zn/N co-doped TiO_2 nanotube upon simulated solar light irradiation reveals that the complete degradation of PCP solutions is obtained after 110 and 100 minutes, respectively, demonstrating the more time required for 100% treatment of PCP in a sample prepared of agricultural wastewater that is associated with the presence of more PCP and organic compound molecules in agricultural wastewater. Furthermore, it is indicated that the successful application of the developed photocatalyst for PCP degradation in an agricultural waste sample.

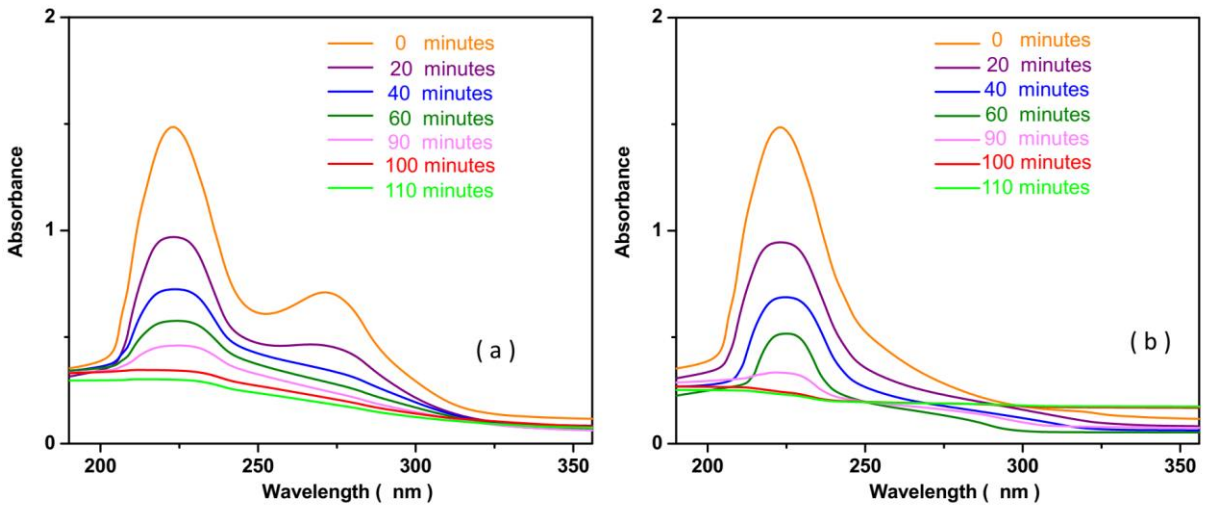

Figure 7. UV–Vis spectra of photodegradation of 50 ml of 10 mg/l PCP solution prepared from (a) real sample of agricultural wastewater and (b) deionized water with respect to different irradiation times.

4. CONCLUSION

This study presented the synthesis of iO_2, Zn/TiO_2, N/TiO_2 and Zn/N co-doped TiO_2 nanotubes and their application for the photocatalytic degradation of PCP. The nanotubes were synthesized by the sol-gel method, and structural studies indicated successful mono-doping and co-doping of TiO_2 nanotubes. Results of optical studies revealed that the optical band gap values of TiO_2, Zn/TiO_2, N/TiO_2 and Zn/N co-doped TiO_2 nanotubes were estimated at 3.29, 3.25, 3.21 and 3.16 eV, respectively. Results of EIS analyses showed that Zn/N co-doped TiO_2 nanotubes with the lowest charge transfer resistance towards pure and mono-doped TiO_2 can accelerate the interfacial photo-

excited charge carrier transfer rate. Studying the photocatalytic activity of prepared photocatalyst for degradation of 50 ml of 40 mg/l PCP solution upon simulated solar light irradiation showed that the time required of TiO_2, N/TiO_2, Zn/TiO_2 and Zn/N co-doped TiO_2 nanotubes for complete degradation of PCP molecules were 250, 200, 185 and 155 minutes, respectively. The highest rate of photodegradation of PCP solution was observed for the co-doped TiO_2 nanotubes.

ACKNOWLEDGEMENT
This research was supported by the Science and Technology Research Plan of Liaoning Province Education Department [L2020lkyfwdf-06].

References

1. K. Ravichandran, C. Dhanraj and P. Kavitha, *Surfaces and Interfaces*, 20 (2020) 100629.
2. B. Bai, Q. Nie, H. Wu and J. Hou, *Powder Technology*, 394 (2021) 1158.
3. X.-Q. Lin, Z.-L. Li, B. Liang, H.-L. Zhai, W.-W. Cai, J. Nan and A.-J. Wang, *Water research*, 162 (2019) 236.
4. H. Maleh, M. Alizadeh, F. Karimi, M. Baghayeri, L. Fu, J. Rouhi, C. Karaman, O. Karaman and R. Boukherroub, *Chemosphere*, (2021) 132928.
5. R.S. Singh, T. Singh and A. Pandey, *Advances in enzyme technology*, 25 (2019) 1.
6. H. Liu, X. Li, Z. Ma, M. Sun, M. Li, Z. Zhang, L. Zhang, Z. Tang, Y. Yao and B. Huang, *Nano Letters*, 21 (2021) 10284.
7. S. Khosravi and S.M.M. Dezfouli, *Journal of Critical Reviews*, 7 (2020) 275.
8. C. Zhao, M. Xi, J. Huo, C. He and L. Fu, *Materials Today Physics*, 22 (2022) 100609.
9. D. Ge, H. Yuan, J. Xiao and N. Zhu, *Science of The Total Environment*, 679 (2019) 298.
10. Y.-M. Chu, U. Nazir, M. Sohail, M.M. Selim and J.-R. Lee, *Fractal and Fractional*, 5 (2021) 119.
11. B. Zhang, Y. Cheng, J. Shi, X. Xing, Y. Zhu, N. Xu, J. Xia and A.G. Borthwick, *Chemical Engineering Journal*, 375 (2019) 121965.
12. S. Mu, Q. Liu, P. Kidkhunthod, X. Zhou, W. Wang and Y. Tang, *National science review*, 8 (2021) nwaa178.
13. A. Roghani, *AIMS Public Health*, 8 (2021) 655.
14. R. Deng, Y. Zhu, J. Hou, J.C. White, J.L. Gardea-Torresdey and D. Lin, *Carbon*, 145 (2019) 658.
15. D. Xu and H. Ma, *Journal of Cleaner Production*, 313 (2021) 127758.
16. K.A. Zahidah, S. Kakooei, M. Kermanioryani, H. Mohebbi, M.C. Ismail and P.B. Raja, *International Journal of Engineering and Technology Innovation*, 7 (2017) 243.
17. B. Bai, S. Jiang, L. Liu, X. Li and H. Wu, *Powder Technology*, 387 (2021) 22.
18. W. Liu, Y. Zheng, Z. Wang, Z. Wang, J. Yang, M. Chen, M. Qi, S. Ur Rehman, P.P. Shum and L. Zhu, *Advanced Materials Interfaces*, 8 (2021) 2001978.
19. M. Khosravi, *Psychiatry*, 27 (2019) 171.
20. Z. Heidari, M. Motevasel and N.A. Jaafarzadeh, *Iranian Journal of Oil and Gas Science and Technology*, 4 (2015) 76.
21. W. Jianlong, Q. Yi, N. Horan and E. Stentiford, *Bioresource Technology*, 75 (2000) 157.
22. E. Kim, H. Chae and K. Chu, *Journal of Environmental Sciences*, 19 (2007) 1032.
23. Y. Li, J. Niu, L. Yin, W. Wang, Y. Bao, J. Chen and Y. Duan, *Journal of Environmental Sciences*, 23 (2011) 1911.

24. H. Zhao, Y. Chen, X. Quan and X. Ruan, *Chinese Science Bulletin*, 52 (2007) 1456.
25. T.T. ThanhThuy, H. Feng and Q. Cai, *Chemical Engineering Journal*, 223 (2013) 379.
26. J. Rouhi, S. Mahmud, S. Hutagalung and S. Kakooei, *Micro & Nano Letters*, 7 (2012) 325.
27. S. Vaziri, R. Mosaddegh, M. Rezai, F. Mohammadi and M.A. Ashari, *Journal of Critical Reviews*, 7 (2019) 2020.
28. H.R. Pouretedal, *Journal of Alloys and Compounds*, 735 (2018) 2507.
29. L. Yang, L. Li, L. Li, C. Liu, J. Li, B. Lai and N. Li, *RSC Advances*, 11 (2021) 4942.
30. G.S. Garbellini, G.R. Salazar-Banda and L.A. Avaca, *Portugaliae Electrochimica Acta*, 28 (2010) 405.
31. Y.-M. Chu, B. Shankaralingappa, B. Gireesha, F. Alzahrani, M.I. Khan and S.U. Khan, *Applied Mathematics and Computation*, 419 (2022) 126883.
32. L. Yu and B. Tang, *International Journal of Electrochemical Science*, 16 (2021) 210915.
33. B. Han, X. Wei and R. Gu, *International Journal of Electrochemical Science*, 16 (2021) 210618.
34. N.Ç. Bezir, A. Evcin, R. Diker, B. Özcan, E. Kır, G. Akarca, E.S. Çetin, R. Kayalı and M.K. Özen, *Open Chemistry*, 16 (2018) 732.
35. A. Ashfaq, M. Ikram, A. Haider, A. Ul-Hamid, I. Shahzadi and J. Haider, *Nanoscale Research Letters*, 16 (2021) 1.
36. H. Savaloni and R. Savari, *Materials Chemistry and Physics*, 214 (2018) 402.
37. R. Mosaddegh, N. Ashayeri, M. Rezai, G. Masoumi, S. Vaziri, F. Mohammadi, H. Givzadeh and N. Noohi, *Open access emergency medicine: OAEM*, 11 (2019) 9.
38. M. Ahamed, M.A.M. Khan, M.J. Akhtar, H.A. Alhadlaq and A. Alshamsan, *Scientific Reports*, 6 (2016) 30196.
39. Y. Liu, Q. Zhang, H. Yuan, K. Luo, J. Li, W. Hu, Z. Pan, M. Xu, S. Xu and I. Levchenko, *Journal of Alloys and Compounds*, 868 (2021) 158723.
40. A. Bahrami, S. Jafarnejad, H. khoshnezhad Ebrahimi, S.M.M. Dezfouli and R. Pahlevani, *Systematic Reviews in Pharmacy*, 11 (2020) 905.
41. Z. Zhang, Y. Yang and D. Cheng, *International Journal of Electrochemical Science*, 16 (2021) 21115.
42. G. Nagaraj, A. Irudayaraj and R. Josephine, *Optik*, 179 (2019) 889.
43. F. Tavakoli and A. Badiei, *Pollution*, 4 (2018) 687.
44. S. Pang, J.g. Huang, Y. Su, B. Geng, S.y. Lei, Y.t. Huang, C. Lyu and X.j. Liu, *Photochemistry and photobiology*, 92 (2016) 651.
45. R. Hassanzadeh, A. Siabi-Garjan, H. Savaloni and R. Savari, *Materials Research Express*, 6 (2019) 106429.
46. M. Chekini, M. Mohammadizadeh and S.V. Allaei, *Applied Surface Science*, 257 (2011) 7179.
47. P. Karimian and M.A. Delavar, *Pakistan Journal of Medical & Health Sciences*, 14 (2020) 1405.
48. C. Zhao, G. Tan, W. Yang, C. Xu, T. Liu, Y. Su, H. Ren and A. Xia, *Scientific Reports*, 6 (2016) 38603.
49. M. Nazeer, F. Hussain, M.I. Khan, E.R. El-Zahar, Y.-M. Chu and M. Malik, *Applied Mathematics and Computation*, 420 (2022) 126868.
50. M. Ismail, M.M. Chebaane, L. Bousselmi, O. Zahraa, C. Olivier and T. Toupance, *Surfaces and Interfaces*, 27 (2021) 101543.
51. F. Husairi, J. Rouhi, K. Eswar, C.R. Ooi, M. Rusop and S. Abdullah, *Sensors and Actuators A: Physical*, 236 (2015) 11.
52. X. Kang, S. Liu, Z. Dai, Y. He, X. Song and Z. Tan, *Catalysts*, 9 (2019) 191.
53. A.O. Ibhadon and P. Fitzpatrick, *Catalysts*, 3 (2013) 189.
54. R.K. Mulpuri, S.R. Tirukkovalluri, M.R. Imandi, S.A. Alim and V.D.L. Kapuganti, *Sustainable Environment Research*, 29 (2019) 1.

55. T.H. Zhao, M.I. Khan and Y.M. Chu, *Mathematical Methods in the Applied Sciences*, (2021)
56. S.M.M. Dezfouli and S. Khosravi, *Indian Journal of Forensic Medicine and Toxicology*, 15 (2021) 2674.
57. P. Makal and D. Das, *Applied Surface Science*, 455 (2018) 1106.
58. K. Eswar, J. Rouhi, H. Husairi, M. Rusop and S. Abdullah, *Advances in Materials Science and Engineering*, 2014 (2014) 1.
59. H. Savaloni, E. Khani, R. Savari, F. Chahshouri and F. Placido, *Applied Physics A*, 127 (2021) 1.
60. H. Savaloni, R. Savari and S. Abbasi, *Current Applied Physics*, 18 (2018) 869.
61. J. Gunlazuardi and W.A. Lindu, *Journal of Photochemistry and Photobiology A: Chemistry*, 173 (2005) 51.
62. X. Quan, X. Ruan, H. Zhao, S. Chen and Y. Zhao, *Environmental Pollution*, 147 (2007) 409.
63. Z. Gao, S. Yang, C. Sun and J. Hong, *Separation and Purification Technology*, 58 (2007) 24.